Vietnam Journal of Mechanics, Vietnam Academy of Science and Technology
DOI: https://doi.org/10.15625/0866-7136/23918

FORCED VIBRATION ANALYSIS OF CRACKED CONTINUOUS MULTI-SPAN FUNCTIONALLY GRADED NANOBEAMS

Tran Van Lien, Tran Binh Dinh*
Hanoi University of Civil Engineering, Hanoi, Vietnam
*E-mail: dinhtb@huce.edu.vn

Received: 08 December 2025 / Revised: 07 January 2026 / Accepted: 10 January 2026
Published online: 28 March 2026

Abstract. The paper analyses the forced vibration of cracked continuous multi-span functionally graded nanobeams based on the nonlocal elasticity theory (NET), Euler–Bernoulli beam theory (EBT), and the dynamic stiffness method (DSM). The NET accounts for the nanoscale size effect of the structure. A crack model using three springs with stiffness dependent on the crack depth is proposed. The equations of motion are derived using Hamilton's principle, NET, and EBT. Various boundary conditions are formulated from the weak form of the equations of motion, thereby overcoming the nonlocal paradox. The reliability of the proposed method is verified through comparison with published results. The effects of geometric, material, nonlocal, and crack parameters on the forced vibration behaviour of continuous multi-span nanobeams are analysed in detail.

Keywords: cracks, FGM, nanobeam, nonlocal, weak form.

1. INTRODUCTION

Functionally graded materials (FGMs) are a new generation of composite materials whose constituents vary continuously in one or more directions to reduce stress concentration and enhance the bonding strength between different material layers. At present, FGMs are widely used in beam and plate structures of NEMS/MEMS devices and in various high-tech engineering applications.

In nanostructures, damage or cracks may occur due to atomic vacancies (Ghadiri et al., 2016) or thermal expansion during fabrication (Kirkham et al., 2008). The complexity of fracture mechanics problems in FGM materials (Erdogan & Wu, 1997; Jin & Batra, 1996), as well as the dynamic analysis of cracked FGM nanostructures, are the main reasons why studies on the vibration behaviour of damaged structures remain limited.

Using Eringen's nonlocal elasticity theory (NET) (Eringen, 2002), several studies have investigated cracked homogeneous nanobeams under various boundary conditions (Loya et al., 2009; Roostai & Haghpanahi, 2014; Torabi & Dastgerdi, 2012), stepped nanobeams with multiple cracks (M. Hossain & Lellep, 2020; Lellep & Lenbaum, 2016, 2018; Lellep & Lenbaum, 2019; Loghmani & Yazdi, 2018), and the effects of elastic foundations (M. M. Hossain & Lellep, 2021) or environmental temperature (Abdullah et al., 2021; Aria et al., 2019; Ebrahimi & Mahmoodi, 2018; Karličić et al., 2015). However, very few studies have focused on the free and forced vibration of cracked FGM nanobeams. Soltanpour et al. (2017) analysed the free vibration of cracked FGM nanobeams resting on a polymer elastic foundation. Ghadiri et al. (2016) examined the effect of surface energy on the free vibration of cracked Timoshenko FGM nanobeams on an elastic

foundation. Esen et al. (2021) investigated the vibration of cracked microbeams on an elastic foundation under magnetic and thermal fields. All of these studies mainly considered simply supported or cantilever FGM nanobeams with a single crack.

Due to inconsistencies in formulating nonlocal boundary conditions, the NET has led to the so-called *nonlocal paradox* (Ghavanloo et al., 2019; Li & Wang, 2009). To address this issue, Challamel et al. (2014) proposed a beam discretization model, while Khodabakhshi and Reddy (2015) introduced a unified integro-differential nonlocal model to replace the continuous one. Xu et al. (2016) employed the weighted residual method for homogeneous beams, and Aria and Friswell (2019) combined it with the finite element method. Meanwhile, Lien et al. (2024) and Tran et al. (2023) proposed applying the weighted residual method together with the dynamic stiffness method (DSM) to obtain accurate boundary conditions for FGM nanobeams.

This paper presents the forced vibration analysis of cracked continuous multi-span FGM nanobeams based on the NET, EBT, and the DSM. The remainder of the paper is organized as follows: Section 2 presents the solution for the forced vibration of intact FGM nanobeams. Section 3 introduces the cracked nanobeam element model, in which each crack is represented by three equivalent springs derived from fracture mechanics. Section 4 provides the exact solution for multi-cracked FGM nanobeams subjected to external loads using the DSM. Section 5 presents numerical studies and discussions. Finally, the conclusions summarize the main findings and offer recommendations drawn from this study.

2. THE SOLUTION OF THE FORCED VIBRATION PROBLEM OF AN INTACT FGM NANOBEAM

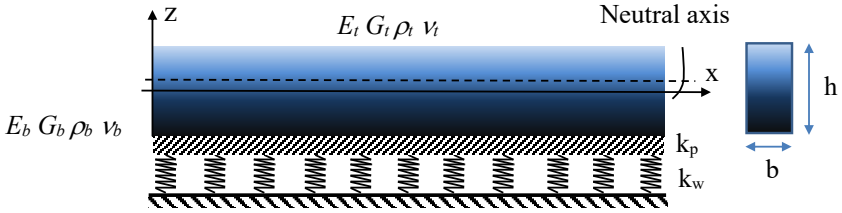

Fig. 1. A nanobeam on a Winkler–Pasternak elastic foundation

Consider an FGM nanobeam with material properties varying along its height as follows (Shen, 2016):

$$\{E(z),\ \rho(z)\}^T = \{E_b, \rho_b\}^T + \{E_t - E_b, \rho_t - \rho_b\}^T \left(z/h + 0.5\right)^n, \tag{1}$$

where E and ρ are the elastic modulus and mass density, respectively; the subscripts t and b denote the top and bottom layers, and n is the volume fraction index (Fig. 1). The displacement of the beam according to the EBT is expressed as follows:

$$u(x,z,t) = u_0(x,t) - (z - h_0)\, w_{0,x}(x,t), \quad w(x,z,t) = w_0(x,t), \tag{2}$$

where $u(x,t)$ is the axial displacement; $w(x,t)$ is the deflection of a point on the neutral axis; h_0 is the distance from the neutral axis to the x axis. Following Eltaher et al. (2014), the position of the neutral axis was determined under the assumption that the axial displacement and nonlocal effects are neglected

$$h_0 = \frac{nh(R_E - 1)}{2(n+2)(n+R_E)}, \quad R_E = \frac{E_t}{E_b}. \tag{3}$$

In the frequency domain, the vibration equation of an intact FGM nanobeam based on the EBT (Hung et al., 2023) is given as follows:

$$[\mathbf{A}_0]\left\{\frac{\mathrm{d}^4\mathbf{z}}{\mathrm{d}x^4}\right\} + [\mathbf{A}_1]\left\{\frac{\mathrm{d}^3\mathbf{z}}{\mathrm{d}x^3}\right\} + [\mathbf{A}_2]\left\{\frac{\mathrm{d}^2\mathbf{z}}{\mathrm{d}x^2}\right\} + [\mathbf{A}_3]\left\{\frac{\mathrm{d}\mathbf{z}}{\mathrm{d}x}\right\} + [\mathbf{A}_4]\{\mathbf{z}\} = -\{\mathbf{q}\}. \tag{4}$$

The boundary conditions are derived from the weak form of the equation of motion

$$\begin{pmatrix} N & M & Q \end{pmatrix}^T = [\mathbf{b}_F]\{\mathbf{z}\} - \mu\{\tilde{\mathbf{Q}}\}, \tag{5}$$

where $[\mathbf{A}_0], [\mathbf{A}_1], [\mathbf{A}_2], [\mathbf{A}_3], [\mathbf{A}_4], \{\mathbf{z}\}, \{\mathbf{q}\}, \{\tilde{\mathbf{Q}}\}$ are the matrices

$$\begin{aligned}
&[\mathbf{A}_0] = \begin{pmatrix} 0 & 0 \\ 0 & A_{22} - \mu\left(I_{22}\omega^2 - k_p\right) \end{pmatrix}, \quad [\mathbf{A}_1] = \begin{pmatrix} 0 & -\left(A_{12} - \mu I_{12}\omega^2\right) \\ -\left(A_{12} - \mu I_{12}\omega^2\right) & 0 \end{pmatrix}, \\
&[\mathbf{A}_2] = \begin{pmatrix} A_{11} - \mu\left(I_{11}\omega^2 - k_u\right) & 0 \\ 0 & I_{22}\omega^2 - k_p + \mu\left(I_{11}\omega^2 - k_w\right) \end{pmatrix}, \\
&[\mathbf{A}_3] = \begin{pmatrix} 0 & -I_{12}\omega^2 \\ -I_{12}\omega^2 & 0 \end{pmatrix}, \quad [\mathbf{A}_4] = \begin{pmatrix} I_{11}\omega^2 - k_u & 0 \\ 0 & -\left(I_{11}\omega^2 - k_w\right) \end{pmatrix}, \\
&\{\mathbf{z}\} = \begin{Bmatrix} U \\ W \end{Bmatrix}, \quad \begin{Bmatrix} \tilde{P}(x,\omega) \\ \tilde{Q}(x,\omega) \end{Bmatrix} = \int_{-\infty}^{\infty} \begin{Bmatrix} p(x,t) \\ q(x,t) \end{Bmatrix} e^{-i\omega t}\,\mathrm{d}t, \\
&\{\mathbf{q}\} = \begin{Bmatrix} \tilde{P} - \mu\dfrac{\mathrm{d}^2\tilde{P}}{\mathrm{d}x^2} \\ -\tilde{Q} + \mu\dfrac{\mathrm{d}^2\tilde{Q}}{\mathrm{d}x^2} \end{Bmatrix}, \quad \{\tilde{\mathbf{Q}}\} = \begin{pmatrix} \dfrac{\mathrm{d}\tilde{P}}{\mathrm{d}x} \\ \tilde{Q} \\ \dfrac{\mathrm{d}\tilde{Q}}{\mathrm{d}x} \end{pmatrix},
\end{aligned} \tag{6}$$

$[\mathbf{b}_F]$ is the boundary condition operator

$$[\mathbf{b}_F] = \begin{bmatrix} \left[A_{11} - \mu\left(I_{11}\omega^2 - k_u\right)\right]\partial_x & -\left(A_{12} - \mu I_{12}\omega^2\right)\partial_x^2 \\ \left(A_{12} - \mu I_{12}\omega^2\right)\partial_x & -\mu\left(I_{11}\omega^2 - k_w\right) - \left[A_{22} - \mu\left(I_{22}\omega^2 - k_p\right)\right]\partial_x^2 \\ I_{12} + \left(A_{12} - \mu I_{12}\omega^2\right)\partial_x^2 & -\left[I_{22}\omega^2 + \mu\left(I_{11}\omega^2 - k_w\right)\right]\partial_x - \left[A_{22} - \mu\left(I_{22}\omega^2 - k_p\right)\right]\partial_x^3 \end{bmatrix}, \tag{7}$$

K_u, K_w and K_p are the Winkler–Pasternak foundation coefficients corresponding to the axial and transverse displacements, respectively; A_{11}, A_{12}, and A_{22} are the stiffness coefficients, respectively; I_{11}, I_{12}, and I_{22} are the mass moments, respectively

$$\begin{aligned}
(A_{11}, A_{12}, A_{22}) &= \int_A E(z)\left[1, z - h_0, (z - h_0)^2\right]\mathrm{d}A, \\
(I_{11}, I_{12}, I_{22}) &= \int_A \rho(z)\left[1, z - h_0, (z - h_0)^2\right]\mathrm{d}A.
\end{aligned} \tag{8}$$

The general solution for the free vibration problem of an EBT FGM nanobeam is given as follows:

$$\{\mathbf{Z}_0(x,\omega)\} = \left\{U, W, W', W''\right\}^T = [\mathbf{G}]\{\mathbf{C}\}, \tag{9}$$

where $\{\mathbf{C}\} = (C_1, ..., C_6)^T$ is the constant vector determined from the boundary conditions; $\mathbf{G}$ is the matrix as follows:

$$[\mathbf{G}] = \begin{pmatrix} \alpha_1 e^{k_1 x} & \alpha_2 e^{k_2 x} & \alpha_3 e^{k_3 x} & -\alpha_1 e^{-k_1 x} & -\alpha_2 e^{-k_2 x} & -\alpha_3 e^{-k_3 x} \\ e^{k_1 x} & e^{k_2 x} & e^{k_3 x} & e^{-k_1 x} & e^{-k_2 x} & e^{-k_3 x} \\ k_1 e^{k_1 x} & k_2 e^{k_2 x} & k_3 e^{k_3 x} & -k_1 e^{-k_1 x} & -k_2 e^{-k_2 x} & -k_3 e^{-k_3 x} \\ k_1^2 e^{k_1 x} & k_2^2 e^{k_2 x} & k_3^2 e^{k_3 x} & k_1^2 e^{-k_1 x} & k_2^2 e^{-k_2 x} & k_3^2 e^{-k_3 x} \end{pmatrix}, \tag{10}$$

α_j $(j = 1, 2, 3)$ are the coefficients

$$\alpha_j = k_j \frac{\left(A_{12} - \mu I_{12}\omega^2\right) k_j^2 + I_{12}\omega^2}{\left(A_{11} - \mu I_{11}\omega^2\right) k_j^2 + I_{11}\omega^2 - k_w}, \tag{11}$$

$k_j = \sqrt{\lambda_j}$ and λ_j are the roots of the characteristic equation

$$\det\left(\lambda^4 \left[\mathbf{A}_0\right] + \lambda^3 \left[\mathbf{A}_1\right] + \lambda^2 \left[\mathbf{A}_2\right] + \lambda \left[\mathbf{A}_3\right] + \left[\mathbf{A}_4\right]\right) = 0. \tag{12}$$

The solution of Eq. (4) under external loading $\{\mathbf{q}\}$ is expressed as follows:

$$\left\{\mathbf{z}_q(x,\omega)\right\} = \int_0^x \left[\mathbf{H}(x-\tau,\omega)\right] \left\{\mathbf{q}(\tau,\omega)\right\} \mathrm{d}\tau, \tag{13}$$

where $[\mathbf{H}(x,\omega)]$ is the transfer function matrix that satisfies the equation

$$\left[\mathbf{A}_0\right] \left\{\frac{\mathrm{d}^4\mathbf{H}}{\mathrm{d}x^4}\right\} + \left[\mathbf{A}_1\right] \left\{\frac{\mathrm{d}^3\mathbf{H}}{\mathrm{d}x^3}\right\} + \left[\mathbf{A}_2\right] \left\{\frac{\mathrm{d}^2\mathbf{H}}{\mathrm{d}x^2}\right\} + \left[\mathbf{A}_3\right] \left\{\frac{\mathrm{d}\mathbf{H}}{\mathrm{d}x}\right\} + \left[\mathbf{A}_4\right] \left\{\mathbf{H}\right\} = \left\{\mathbf{0}\right\}, \tag{14}$$

and the boundary conditions at the left node

$$\left[\mathbf{H}(0)\right] = [0], \quad \left[\mathbf{H}'(0)\right] = [0], \quad \left[\mathbf{H}''(0)\right] = [0], \quad \left[\mathbf{H}'''(0)\right] = \left[\mathbf{A}_0\right]^{-1}. \tag{15}$$

3. THE MULTIPLE CRACKED FGM NANOBEAM ELEMENT

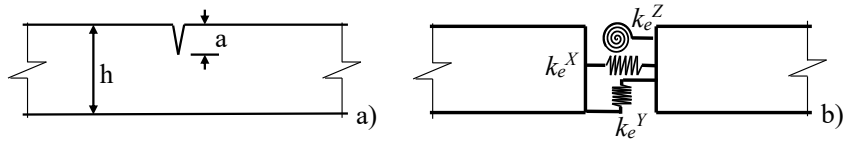

Fig. 2. An FGM nanobeam with an open crack and an equivalent three-spring model

For an FGM nanobeam, a crack located at $z = e$ is modelled by an axial spring with stiffness k_e^X, a rotational spring with stiffness k_e^Z, and a shear spring with stiffness k_e^Y which connect the two intact segments at the crack section (Fig. 2). The continuity conditions at the cracked section are given (Khiem & Huyen, 2017; Yokoyama & Chen, 1998)

$$\begin{aligned} &U(e+0) - U(e-0) = \gamma_1 U'(e), \quad W(e+0) - W(e-0) = -\gamma_3 W'''(e), \\ &W'(e+0) - W'(e-0) = -\gamma_2 W''(e), \quad U'(e+0) = U'(e-0) = U'(e), \\ &W''(e+0) = W''(e-0) = W''(e), \quad W'''(e+0) = W'''(e-0) = W'''(e), \end{aligned} \tag{16}$$

with

$$\gamma_1 = A_{11} \Big/ k_e^X, \quad \gamma_2 = A_{22} \Big/ k_e^Z, \quad \gamma_3 = A_{22} \Big/ k_e^Y. \tag{17}$$

Crack parameters γ_1, γ_2, γ_3 depend on the elastic modulus, Poisson's ratio, the volume fraction index, the beam height, the crack depth, etc., similar to the case of a beam made of homogeneous material. Crack parameters are calculated from the crack depth as follows (Chondros et al., 1998a, 1998b; Yokoyama & Chen, 1998):

$$\gamma_1 = 2\pi(1-\nu^2)h\sigma_1 f_1(s), \quad \gamma_2 = 6\pi(1-\nu^2)h\sigma_2 f_2(s), \quad \gamma_3 = 2\pi(1-\nu^2)h\sigma_2 f_3(s), \tag{18}$$

where $s = a/h$; σ_1 and σ_2 are functions of FGM material parameters (Khiem & Huyen, 2017)

$$\sigma_1 = \frac{2(R_e+n)}{(R_e+1)(1+n)}, \quad R_e = \frac{E_t}{E_b}, \quad \sigma_2 = \frac{24}{R_e+1}\left[\frac{3R_e+n}{3(3+n)} - \frac{2R_e+n}{2+n}\alpha + \frac{R_e+n}{1+n}\alpha^2\right], \tag{19}$$

and f_1, f_2, and f_3 are experimental functions obtained from classical fracture mechanics (Chondros et al., 1998a, 1998b; Yokoyama & Chen, 1998)

$$\begin{aligned} f_1(s) &= 0.6272s^2 - 0.17248s^3 + 5.92134s^4 - 10.7054s^5 + 31.5685s^6 \\ &\quad - 67.47s^7 + 139.123s^8 - 146.682s^9 + 92.3552s^{10}, \\ f_2(s) &= 0.6272s^2 - 1.04533s^3 + 4.5948s^4 - 9.9736s^5 + 20.2948s^6 \\ &\quad - 33.0351s^7 + 47.1063s^8 - 40.7556s^9 + 19.6s^{10}, \\ f_3(s) &= -2.1668\log(1-s) - 2.1668s - 1.0834s^2 + 0.6018s^3 \\ &\quad + 4.9485s^4 + 0.4461s^5 - 10.9659s^6 + 9.3162s^7 - 2.5110s^8. \end{aligned} \tag{20}$$

The solution of Eq. (4) without the right-hand side can be expressed as follows:

$$\{\mathbf{Z}_c(x,\omega)\} = [\mathbf{G}_c(x,\omega)]\{\mathbf{Z'}_0(e)\}, \tag{21}$$

where $\{\mathbf{Z'}_0(e)\} = \left(U_0'(e) \;\; W_0'(e) \;\; W_0''(e) \;\mathbf{W}_0'''(e)\right)^T$ and $[\mathbf{G}_c(x,\omega)]$ is a particular solution that satisfies the initial condition (16). Therefore, the solution of Eq. (4) without the right-hand side for a nanobeam with a single crack is

$$\{\mathbf{z}_c(x,\omega)\} = \{\mathbf{z}_0(x,\omega)\} + [\mathbf{G}_C(x-e,\omega)]\left\{\mathbf{z'}_0(e)\right\}, \tag{22}$$

in which the first term is the solution of an intact FGM nanobeam, and the second term is the solution of a nanobeam with a crack located at a distance e. Using the recurrence relation, the solution of Eq. (4) for a nanobeam with multiple cracks can be expressed as follows:

$$\{\mathbf{z}_c(x,\omega)\} = \left([\mathbf{G}(x,\omega)] + \sum_{j=1}^{n}\left[\mathbf{G}_C(x-e_j)\right]\left[\bar{\chi}_j\right]\right)\{\mathbf{C}\} = \left[\bar{\mathbf{\Psi}}(x,\omega)\right]\{\mathbf{C}\}, \tag{23}$$

where $\left[\bar{\chi}_j\right]$ is a constant matrix

$$\left[\bar{\chi}_j\right] = \left[\mathbf{G'}(e_j)\right] + \sum_{k=1}^{j-1}\left[\mathbf{G'}_C(e_j-e_k)\right]\left[\bar{\chi}_k\right], \quad j = 1,2,3,...,n. \tag{24}$$

The general solution of Eq. (4) for a nanobeam with multiple cracks under external loading is

$$\{\mathbf{z}_c(x,\omega)\} = \left[\bar{\mathbf{\Psi}}(x,\omega)\right]\{\mathbf{C}\} - \left\{\mathbf{z}_q(x,\omega)\right\}. \tag{25}$$

4. THE EXACT SOLUTION FOR A CRACKED CONTINUOUS MULTI-SPAN FGM NANOBEAM UNDER APPLIED LOADING

Consider an FGM nanobeam element (Fig. 3) with the following nodal displacements and forces

$$\left\{\hat{\mathbf{U}}_e\right\} = \{U_1,\Theta_1,W_1,U_2,\Theta_2,W_2\}^T, \quad \{\mathbf{P}_e\} = \{N_1,M_1,Q_1,N_2,M_2,Q_2\}^T, \tag{26}$$

where

$$\begin{aligned} &U_1 = U(0,\omega), \quad \Theta_1 = W'(0,\omega), \quad W_1 = W(0,\omega), \\ &U_2 = U(L,\omega), \quad \Theta_2 = W'(L,\omega), \quad W_2 = W(L,\omega), \\ &\left(N_1 \;\; M_1 \;\; Q_1\right)^T = -\left[\mathbf{B}_F\right]\left(U \;\; W \;\; W' \;\; W''\right)^T\Big|_{x=0} + \mu\left\{\tilde{\mathbf{Q}}_0\right\}, \\ &\left(N_2 \;\; M_2 \;\; Q_2\right)^T = \left[\mathbf{B}_F\right]\left(U \;\; W \;\; W' \;\; W''\right)^T\Big|_{x=L} - \mu\left\{\tilde{\mathbf{Q}}_L\right\}. \end{aligned} \tag{27}$$

To satisfy the first three conditions of (27), the new matrices $\hat{\mathbf{\Psi}}, \hat{\mathbf{Z}}_q$ are constructed by removing the fourth row of the matrices $\bar{\mathbf{\Psi}}, \mathbf{z}_c$ and arranging them in the same order as in

expression (26). Substituting into Eq. (27) yields

$$\begin{aligned}\{\hat{\mathbf{U}}_e\} &= \begin{bmatrix}[\hat{\mathbf{\Psi}}(0,\omega)]\\ [\hat{\mathbf{\Psi}}(L,\omega)]\end{bmatrix}\cdot\{\mathbf{C}\} - \begin{Bmatrix}\{\hat{\mathbf{0}}\}\\ \{\check{\mathbf{Z}}_q(L)\}\end{Bmatrix},\\ \{\mathbf{P}_e\} &= \begin{bmatrix}[-\mathbf{B}_F(\mathbf{\Psi})_{x=0}]\\ [\mathbf{B}_F(\mathbf{\Psi})_{x=L}]\end{bmatrix}\cdot\{\mathbf{C}\} - \begin{Bmatrix}\{-\mathbf{B}_F(\mathbf{Z}_q)_{x=0}\}\\ \{\mathbf{B}_F(\mathbf{Z}_q)_{x=L}\}\end{Bmatrix} + \mu\begin{Bmatrix}\{\tilde{\mathbf{Q}}_0\}\\ -\{\tilde{\mathbf{Q}}_L\}\end{Bmatrix}.\end{aligned} \tag{28}$$

By eliminating the vector $\{\mathbf{C}\}$ in Eq. (28), we obtain

$$[\hat{\mathbf{K}}_e(\omega)]\cdot\{\hat{\mathbf{U}}_e\} = \{\mathbf{P}_e(\omega)\} + \{\hat{\mathbf{F}}_e\}, \tag{29}$$

where $[\hat{\mathbf{K}}_e]$ and $\{\hat{\mathbf{F}}_e\}$ are respectively the dynamic stiffness matrix and the nodal load vector of the FGM nanobeam element with multiple cracks

$$[\hat{\mathbf{K}}_e] = \begin{bmatrix}[-\mathbf{B}_F(\mathbf{\Psi})_{x=0}]\\ [\mathbf{B}_F(\mathbf{\Psi})_{x=L}]\end{bmatrix}\cdot\begin{bmatrix}[\hat{\mathbf{\Psi}}(0,\omega)]\\ [\hat{\mathbf{\Psi}}(L,\omega)]\end{bmatrix}^{-1}, \tag{30}$$

$$\{\hat{\mathbf{F}}_e\} = \begin{Bmatrix}\{-\mathbf{B}_F(\mathbf{Z}_q)_{x=0}\}\\ \{\mathbf{B}_F(\mathbf{Z}_q)_{x=L}\}\end{Bmatrix} - \begin{bmatrix}[-\mathbf{B}_F(\mathbf{\Psi})_{x=0}]\\ [\mathbf{B}_F(\mathbf{\Psi})_{x=L}]\end{bmatrix}\cdot\begin{bmatrix}[\hat{\mathbf{\Psi}}(0,\omega)]\\ [\hat{\mathbf{\Psi}}(L,\omega)]\end{bmatrix}^{-1}\cdot\begin{Bmatrix}\{\hat{\mathbf{0}}\}\\ \{\hat{\mathbf{Z}}_q(L)\}\end{Bmatrix} + \mu\begin{Bmatrix}-\{\tilde{\mathbf{Q}}_0\}\\ \{\tilde{\mathbf{Q}}_L\}\end{Bmatrix}. \tag{31}$$

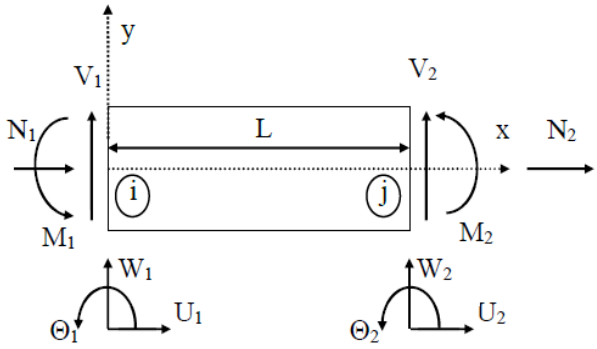

Fig. 3. Nodal displacements and nodal forces

For a beam or frame structure consisting of several FGM nanobeam elements as described above, by enforcing the equilibrium of internal forces at the structural nodes, the global dynamic stiffness matrix $\hat{\mathbf{K}}(\omega)$ and the global nodal force vector $\hat{\mathbf{P}}$ of the entire structure can be obtained. Denoting $\hat{\mathbf{U}}$ as the vector of nodal displacements of the structure, the equation of motion of the structure according to the DSM is given by

$$[\hat{\mathbf{K}}(\omega)]\cdot\{\hat{\mathbf{U}}\} = \{\check{\mathbf{F}}\}. \tag{32}$$

5. RESULTS AND DISCUSSION

In the following computations, the following dimensionless quantities are used

$$\mu^* = \left(\frac{e_0 a}{h}\right)^2, \quad k_w = K_w\frac{12L^4}{E_1 bh^3}, \quad k_p = K_p\frac{12L^2}{E_1 bh^3}. \tag{33}$$

Table 1 presents a comparison of the nondimensional fundamental frequency of a fixed–fixed nanobeam with the results of Reddy (2007) obtained using analytical solutions based on the EBT, Timoshenko beam theory (TBT), Reddy beam theory (RBT), and Levinson beam theory (LBT). The discrepancy is less than 0.1%, demonstrating the reliability of the proposed computational model.

Consider a three-span continuous FGM nanobeam with clamped–fixed supported boundary conditions (Fig. 4) with the following geometric parameters: $b = h = 1\,\text{nm}$, $L = 20h$. The

constituent material consists of a metal with $E_m = 70\,\text{GPa}$, $G_m = 26\,\text{GPa}$, $\rho_m = 2700\,\text{kg/m}^3$, and a ceramic with $E_c = 393\,\text{GPa}$, $G_c = 157\,\text{GPa}$, $\rho_c = 3960\,\text{kg/m}^3$; Poisson's ratio $\nu_m = \nu_c = 0.3$; the volume fraction index $n = 5$. Each beam span contains two cracks with a depth of $0.2h$ located at positions $1h$ and $2h$ from the left end of each span. The beam is subjected to a uniformly distributed load along its entire length with frequency $\omega = 1 \times 10^8\,\text{rad/s}$.

Table 1. Comparison of the first nondimensional frequency of a clamped–clamped nanobeam

μ^*	EBT (Reddy, 2007)	TBT (Reddy, 2007)	RBT (Reddy, 2007)	LBT (Reddy, 2007)	Present
0	9.8696	9.8381	9.8381	9.8433	9.8595
1.0	9.4159	9.3858	9.3858	9.3908	9.4062
2.0	9.0195	8.9907	8.9907	8.9955	9.0102
3.0	8.6693	8.6416	8.6416	8.6462	8.6604
4.0	8.3569	8.3302	8.3302	8.3347	8.3483
5.0	8.0761	8.0503	8.0503	8.0546	8.0678

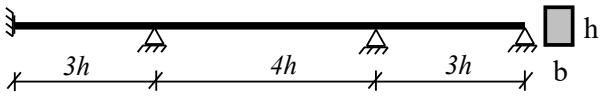

Fig. 4. A three-span continuous FGM nanobeam

Fig. 5 shows the variation of displacement, bending moment, and shear force of a three-span continuous beam with respect to the nonlocal parameter $\mu^* = 0$, 2, 4. The black lines correspond to the uncracked beam, while the red lines correspond to the cracked beam. The solid line represents $\mu^* = 0$, the dashed line $\mu^* = 2$, and the dotted line $\mu^* = 4$. As the nonlocal parameter increases, the displacement in the first and last spans increases, while it decreases in the middle span; at the same time, cracks cause significant changes in displacement across the spans. The effects of cracks and the nonlocal parameter on displacement can be considered roughly equivalent. However, the influence of the nonlocal parameter on bending moment and shear force is more pronounced than that of the cracks.

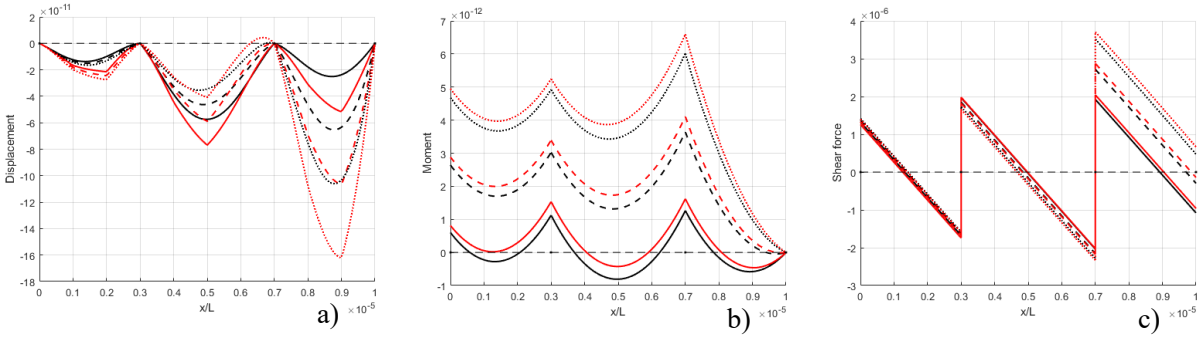

Fig. 5. Variation of displacement (a), bending moment (b), and shear force (c) with $\mu^* = 0, 2, 4$

Fig. 6 illustrates the variation of displacement, bending moment, and shear force of the continuous beam with respect to the volume fraction index $n = 0$, 1, 10. The solid line corresponds to $n = 0$, the dashed line to $n = 1$, and the dotted line to $n = 10$. As the parameter n increases, the displacements at all spans decrease, while the presence of cracks increases the displacement in all three spans. The effects of the crack and the parameter n on displacement

can be considered equivalent. However, when the beam contains cracks, the influence of the parameter n on the bending moment becomes more pronounced than in the uncracked case. The effects of the crack and the parameter n on the shear force are small and can be neglected.

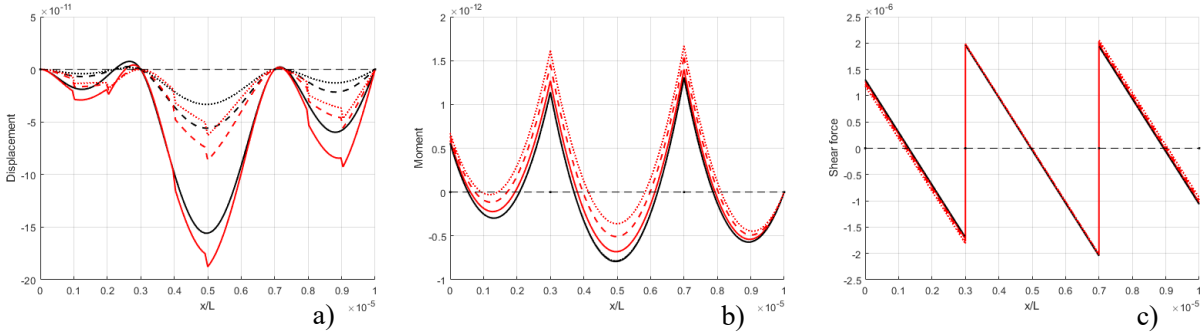

Fig. 6. Variation of displacement (a), bending moment (b), and shear force (c) with $n = 0, 1, 10$

Fig. 7 illustrates the variations in displacement, bending moment, and shear force of the continuous beam corresponding to different ratios of the elastic moduli of the upper and lower layers, $E_c/E_m = 0.5$, $393/70$, and 20. The solid line represents $E_c/E_m = 0.5$, the dashed line corresponds to $E_c/E_m = 393/70$, and the dotted line denotes $E_c/E_m = 20$. As the ratio E_c/E_m increases, the displacement in all spans decreases, while the presence of cracks causes the displacement to increase significantly in all three spans. The effects of the crack and the ratio E_c/E_m on the displacement can be considered comparable. However, when the nanobeam contains a crack, the influence of the ratio E_c/E_m on the bending moment becomes more pronounced than that in the uncracked case. The effects of the crack and the ratio E_c/E_m on the shear force are minor and can be neglected.

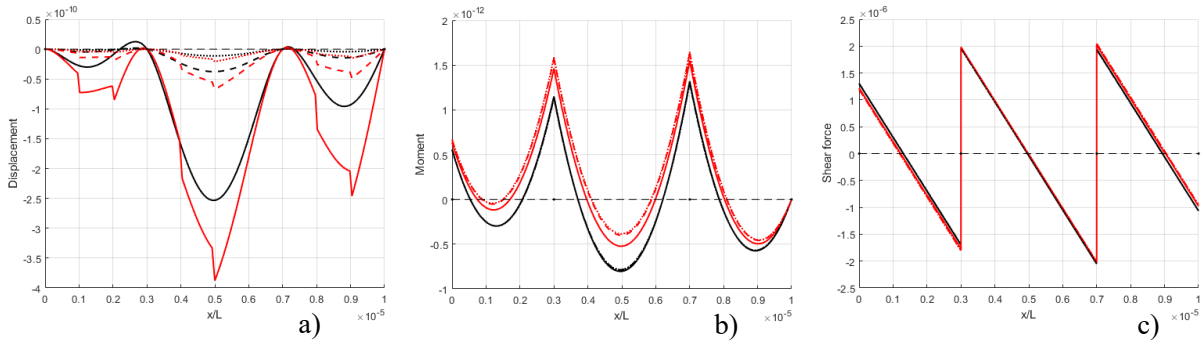

Fig. 7. Variation of displacement (a), moment (b), and shear force (c) with E_c/E_m = 0.5, $393/70$, 20

Fig. 8 illustrates the variations in displacement, bending moment, and shear force of the continuous beam corresponding to different crack depths of $a/h = 0$, 0.2, and 0.4. The solid line represents $a/h = 0$, the dashed line corresponds to $a/h = 0.2$, and the dotted line denotes $a/h = 0.4$. As the ratio a/h increases, the displacement in all spans increases, while the presence of cracks causes the displacement to rise sharply across all three spans. The influence of crack depth on displacement and bending moment is quite significant, whereas its effect on the shear force is small in the outer spans and negligible in the middle span.

Fig. 9 illustrates the variations in displacement, bending moment, and shear force of the continuous beam corresponding to different Winkler foundation stiffness coefficients of $k_w = 0$, 50, and 100. The solid line represents $k_w = 0$, the dashed line corresponds to $k_w = 50$, and the

dotted line denotes $k_w = 100$. It is evident that the influence of the foundation coefficient on the displacement and bending moment is minor compared with the effect of the crack. The effects of the Winkler foundation coefficient and the crack on the shear force are small and can be neglected.

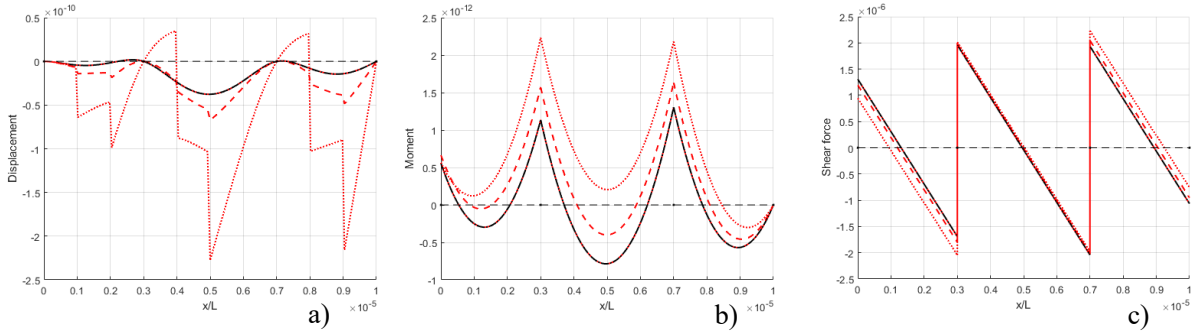

Fig. 8. Variation of displacement (a), bending moment (b), and shear force (c) with $a/h = 0, 0.2, 0.4$

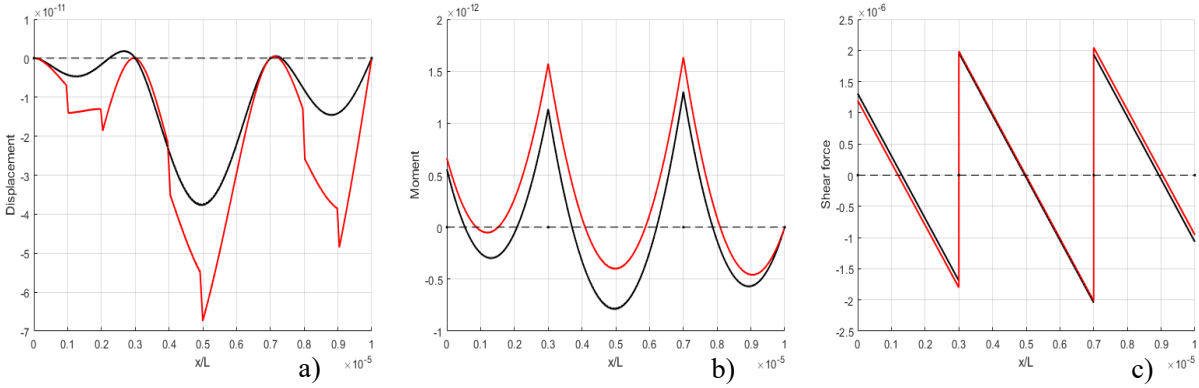

Fig. 9. Variation of displacement (a), bending moment (b), and shear force (c) with $k_w = 0, 50, 100$

Fig. 10 illustrates the variations in displacement, bending moment, and shear force of the continuous beam corresponding to different Pasternak foundation stiffness coefficients of $k_p = 0$, 50, 100. The solid line represents $k_p = 0$, the dashed line corresponds to $k_p = 50$, and the dotted line denotes $k_p = 100$. As the Pasternak foundation coefficient increases, the displacements in all spans decrease, while the presence of cracks causes the displacement to increase significantly in all three spans. The effects of the crack and the foundation coefficient k_p on the displacement can be considered comparable. However, when the beam contains a crack, its influence on the bending moment becomes more pronounced than that of the foundation stiffness coefficient k_p. The effects of the foundation coefficient and the crack on the shear force are minor and can be neglected.

Fig. 11 illustrates the variations in displacement, bending moment, and shear force of the continuous beam corresponding to the external excitation frequencies of $\omega = 1 \times 10^8$, 5×10^8, and 10×10^8 rad/s. The solid line represents $\omega = 1 \times 10^8$ rad/s, the dashed line corresponds to $\omega = 5 \times 10^8$ rad/s, and the dotted line denotes $\omega = 10 \times 10^8$ rad/s. As the excitation frequency increases, the displacement at the midspan increases, whereas the displacements at the first and last spans decrease. Moreover, the presence of cracks causes significant changes in displacement across all three spans. The effects of the crack and excitation frequency on the displacement are found to be comparable. However, when the beam contains a crack, the influence of the crack

on the bending moment becomes more pronounced than that of the excitation frequency. The effects of both the crack and the excitation frequency on the shear force are relatively minor.

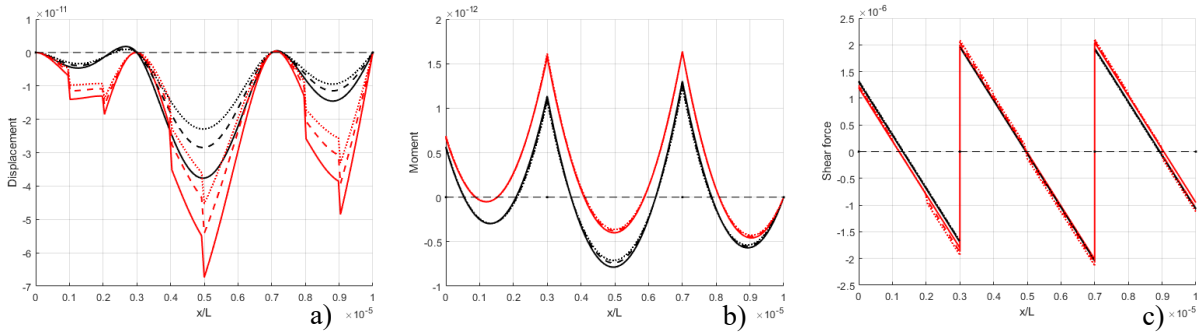

Fig. 10. Variation of displacement (a), bending moment (b), and shear force (c) with $k_p = 0, 50, 100$

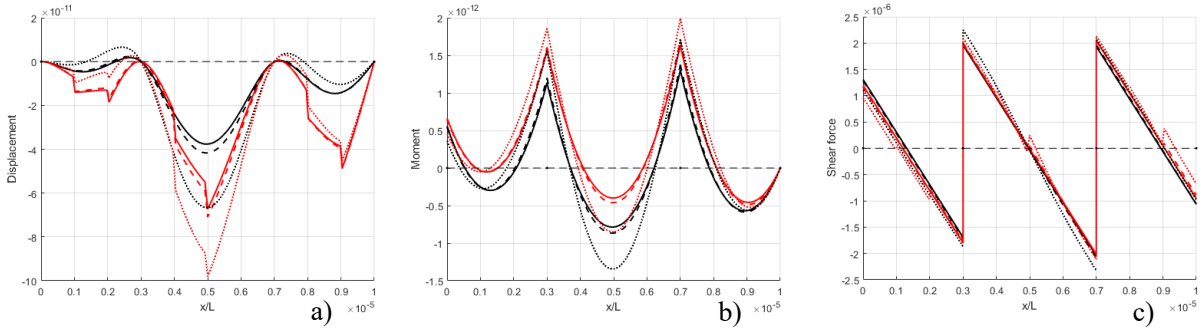

Fig. 11. Variation of displacement (a), bending moment (b), and shear force (c) with respect to the external loading frequency

6. CONCLUSION

In this paper, the authors analysed the forced vibration of multiple cracked continuous multi-span FGM nanobeams using the DSM based on the NET and the EBT. The crack model consists of three springs (an axial spring, a bending spring, and a shear spring), whose stiffness depends on the crack depth according to formulas proposed in fracture mechanics. Accordingly, the effects of geometric, material, and crack parameters on the forced vibration of continuous multi-span FGM nanobeams with multiple cracks are investigated.

The numerical results show that the displacement and bending moment of cracked multi-span FGM nanobeams vary significantly with changes in nonlocal parameters, crack depth, Pasternak foundation parameters, and material properties. The influence of cracks is found to be comparable to that of these parameters in most of the considered cases.

At the crack locations, the displacement exhibits discontinuities, and the rotation angle shows jumps. In the present study, a shear spring associated with the discontinuity of transverse displacement at the cracked cross-section is additionally incorporated. As a result, it is observed that the transverse displacements exhibit not only changes in slope but also displacement jumps. This feature represents a key distinction of the proposed crack model.

All these observations contribute to a better understanding of deformation and displacement in continuous cracked FGM nanobeams. This study can be further extended to other types of FGM materials and more complex nanobeam structures.

DECLARATION OF COMPETING INTEREST

The authors declared no potential conflicting/competing interests with respect to the research, authorship, and/or publication of this article.

CREDIT AUTHOR STATEMENT

Tran Binh Dinh: *Software, Formal analysis, Data curation, Validation, Writing – original draft*. Tran Van Lien: *Conceptualization, Writing – review and editing, Supervision*.

ACKNOWLEDGEMENT

This research was funded by the Ministry of Education and Training under the project code B2025-XDA-05.

REFERENCES

Abdullah, S. S., H. Hashemi, S., A. Hussein, N., & Nazemnezhad, R. (2021). Effect of thermal axial load on vibration of cracked single-walled carbon nanotubes modelled as Timoshenko nanobeams using nonlocal theory. *Australian Journal of Mechanical Engineering*, *21*(3), 860–871. https://doi.org/10.1080/14484846.2021.1918363

Aria, A. I., & Friswell, M. I. (2019). A nonlocal finite element model for buckling and vibration of functionally graded nanobeams. *Composites Part B: Engineering*, *166*, 233–246. https://doi.org/10.1016/j.compositesb.2018.11.071

Aria, A. I., Friswell, M. I., & Rabczuk, T. (2019). Thermal vibration analysis of cracked nanobeams embedded in an elastic matrix using finite element analysis. *Composite Structures*, *212*, 118–128. https://doi.org/10.1016/j.compstruct.2019.01.040

Challamel, N., Zhang, Z., Wang, C. M., Reddy, J. N., Wang, Q., Michelitsch, T., & Collet, B. (2014). On nonconservativeness of Eringen's nonlocal elasticity in beam mechanics: Correction from a discrete-based approach. *Archive of Applied Mechanics*, *84*(9–11), 1275–1292. https://doi.org/10.1007/s00419-014-0862-x

Chondros, T. G., Dimarogonas, A. D., & Yao, J. (1998a). A continuous cracked beam vibration theory. *Journal of Sound and Vibration*, *215*(1), 17–34. https://doi.org/10.1006/jsvi.1998.1640

Chondros, T. G., Dimarogonas, A. D., & Yao, J. (1998b). Longitudinal vibration of a continuous cracked bar. *Engineering Fracture Mechanics*, *61*(5–6), 593–606. https://doi.org/10.1016/s0013-7944(98)00071-x

Ebrahimi, F., & Mahmoodi, F. (2018). Vibration analysis of carbon nanotubes with multiple cracks in thermal environment. *Advances in Nano Research*, *6*(1), 57.

Eltaher, M., Abdelrahman, A., Al-Nabawy, A., Khater, M., & Mansour, A. (2014). Vibration of nonlinear graduation of nano-Timoshenko beam considering the neutral axis position. *Applied Mathematics and Computation*, *235*, 512–529. https://doi.org/10.1016/j.amc.2014.03.028

Erdogan, F., & Wu, B. H. (1997). The surface crack problem for a plate with functionally graded properties. *Journal of Applied Mechanics*, *64*(3), 449–456. https://doi.org/10.1115/1.2788914

Eringen, A. C. (2002). *Nonlocal continuum field theories*. Springer Science & Business Media. https://doi.org/10.1115/1.1553434

Esen, I., Özarpa, C., & Eltaher, M. A. (2021). Free vibration of a cracked FG microbeam embedded in an elastic matrix and exposed to magnetic field in a thermal environment. *Composite Structures*, *261*, 113552. https://doi.org/10.1016/j.compstruct.2021.113552

Ghadiri, M., Soltanpour, M., Yazdi, A., & Safi, M. (2016). Studying the influence of surface effects on vibration behavior of size-dependent cracked FG Timoshenko nanobeam considering nonlocal elasticity and elastic foundation. *Applied Physics A*, *122*(5), 520. https://doi.org/10.1007/s00339-016-0036-5

Ghavanloo, E., Rafii-Tabar, H., & Fazelzadeh, S. A. (2019). *Computational continuum mechanics of nanoscopic structures*. Springer. https://doi.org/10.1007/978-3-030-11650-7

Hossain, M., & Lellep, J. (2020). The effect of rotatory inertia on natural frequency of cracked and stepped nanobeam. *Engineering Research Express*, *2*(3), 035009. https://doi.org/10.1088/2631-8695/aba48b

Hossain, M. M., & Lellep, J. (2021). Mode shape analysis of dynamic behaviour of cracked nanobeam on elastic foundation. *Engineering Research Express*, *3*(4), 045003. https://doi.org/10.1088/2631-8695/ac2a75

Hung, D. T., Lien, T. V., Dinh, T. B., & Thang, N. T. (2023). Free vibration analysis of FGM framed nanostructures using variational-consistent boundary conditions. *Vietnam Journal of Mechanics*, *4*(2). https://doi.org/10.15625/0866-7136/18192

Jin, Z.-H., & Batra, R. C. (1996). Some basic fracture mechanics concepts in functionally graded materials. *Journal of the Mechanics and Physics of Solids*, *44*(8), 1221–1235. https://doi.org/10.1016/0022-5096(96)00041-5

Karličić, D., Jovanović, D., Kozić, P., & Cajić, M. (2015). Thermal and magnetic effects on the vibration of a cracked nanobeam embedded in an elastic medium. *Journal of Mechanics of Materials and Structures*, *10*(1), 43–62. https://doi.org/10.2140/jomms.2015.10.43

Khiem, N. T., & Huyen, N. N. (2017). A method for crack identification in functionally graded Timoshenko beam. *Nondestructive Testing and Evaluation*, *32*(3), 319–341. https://doi.org/10.1080/10589759.2016.1226304

Khodabakhshi, P., & Reddy, J. N. (2015). A unified integro-differential nonlocal model. *International Journal of Engineering Science*, *95*, 60–75. https://doi.org/10.1016/j.ijengsci.2015.06.006

Kirkham, M., Wang, Z. L., & Snyder, R. L. (2008). In situ growth kinetics of ZnO nanobelts. *Nanotechnology*, *19*(44), 445708. https://doi.org/10.1088/0957-4484/19/44/445708

Lellep, J., & Lenbaum, A. (2016). Natural vibrations of a nano-beam with cracks. *International Journal of Theoretical and Applied Mechanics*, *1*(1), 247–252.

Lellep, J., & Lenbaum, A. (2018). Free vibrations of stepped nano-beams. *Computational and Experimental Studies*, 95.

Lellep, J., & Lenbaum, A. (2019). Natural vibrations of stepped nanobeams with defects. *Acta et Commentationes Universitatis Tartuensis de Mathematica*, *23*(1), 143–158. https://doi.org/10.12697/acutm.2019.23.14

Li, X.-F., & Wang, B.-L. (2009). Vibrational modes of Timoshenko beams at small scales. *Applied Physics Letters*, *94*(10), 101903. https://doi.org/10.1063/1.3094130

Lien, T. V., Dinh, T. B., & Thang, N. T. (2024). Exact closed-form solutions for the free vibration analysis of multiple cracked FGM nanobeams. *Proceedings of the Institution of Mechanical Engineers, Part C: Journal of Mechanical Engineering Science*, *238*(8), 3373–3390. https://doi.org/10.1177/09544062231200608

Loghmani, M., & Yazdi, M. R. H. (2018). An analytical method for free vibration of multi cracked and stepped nonlocal nanobeams based on wave approach. *Results in Physics*, *11*, 166–181. https://doi.org/10.1016/j.rinp.2018.08.046

Loya, J., López-Puente, J., Zaera, R., & Fernández-Sáez, J. (2009). Free transverse vibrations of cracked nanobeams using a nonlocal elasticity model. *Journal of Applied Physics*, *105*(4), 044309. https://doi.org/10.1063/1.3068370

Reddy, J. N. (2007). Nonlocal theories for bending, buckling and vibration of beams. *International Journal of Engineering Science*, *45*(2–8), 288–307. https://doi.org/10.1016/j.ijengsci.2007.04.004

Roostai, H., & Haghpanahi, M. (2014). Vibration of nanobeams of different boundary conditions with multiple cracks based on nonlocal elasticity theory. *Applied Mathematical Modelling*, *38*(3), 1159–1169. https://doi.org/10.1016/j.apm.2013.08.011

Shen, H.-S. (2016). *Functionally graded materials: Nonlinear analysis of plates and shells*. CRC Press.

Soltanpour, M., Ghadiri, M., Yazdi, A., & Safi, M. (2017). Free transverse vibration analysis of size dependent Timoshenko FG cracked nanobeams resting on elastic medium. *Microsystem Technologies*, *23*(6), 1813–1830. https://doi.org/10.1007/s00542-016-2983-3

Torabi, K., & Dastgerdi, J. N. (2012). An analytical method for free vibration analysis of Timoshenko beam theory applied to cracked nanobeams using a nonlocal elasticity model. *Thin Solid Films*, *520*(21), 6595–6602. https://doi.org/10.1016/j.tsf.2012.06.063

Tran, L. V., Tran, D. B., & Phan, P. T. T. (2023). Free vibration analysis of stepped FGM nanobeams using nonlocal dynamic stiffness model. *Journal of Low Frequency Noise, Vibration and Active Control*, *42*(3), 997–1017. https://doi.org/10.1177/14613484231160134

Xu, X.-J., Deng, Z.-C., Zhang, K., & Xu, W. (2016). Observations of the softening phenomena in the nonlocal cantilever beams. *Composite Structures*, *145*, 43–57. https://doi.org/10.1016/j.compstruct.2016.02.073

Yokoyama, T., & Chen, M.-C. (1998). Vibration analysis of edge-cracked beams using a line-spring model. *Engineering Fracture Mechanics*, *59*(3), 403–409. https://doi.org/10.1016/s0013-7944(97)80283-4